Bio-Medical Materials and Engineering 26 (2015) S1283–S1290
DOI 10.3233/BME-151426
IOS Press

Pathological brain detection based on wavelet entropy and Hu moment invariants

Yudong Zhang[a,b,*], Shuihua Wang[a,b,*], Ping Sun[c] and Preetha Phillips[d]
[a]*School of Computer Science and Technology, Nanjing Normal University, Nanjing, Jiangsu 210023, China*
[b]*Jiangsu Key Laboratory of 3D Printing Equipment and Manufacturing, Nanjing, Jiangsu 210042, China*
[c]*Department of Electrical Engineering, The City College of New York, CUNY, New York, NY 10031, USA*
[d]*School of Natural Sciences and Mathematics, Shepherd University, Shepherdstown, WV 25443, USA*

Abstract. With the aim of developing an accurate pathological brain detection system, we proposed a novel automatic computer-aided diagnosis (CAD) to detect pathological brains from normal brains obtained by magnetic resonance imaging (MRI) scanning. The problem still remained a challenge for technicians and clinicians, since MR imaging generated an exceptionally large information dataset. A new two-step approach was proposed in this study. We used wavelet entropy (WE) and Hu moment invariants (HMI) for feature extraction, and the generalized eigenvalue proximal support vector machine (GEPSVM) for classification. To further enhance classification accuracy, the popular radial basis function (RBF) kernel was employed. The 10 runs of *k*-fold stratified cross validation result showed that the proposed "WE + HMI + GEPSVM + RBF" method was superior to existing methods w.r.t. classification accuracy. It obtained the average classification accuracies of 100%, 100%, and 99.45% over Dataset-66, Dataset-160, and Dataset-255, respectively. The proposed method is effective and can be applied to realistic use.

Keywords: Wavelet entropy, Hu's moment invariant, magnetic resonance imaging, support vector machine, computer-aided diagnosis, radial basis function

1. Introduction

Magnetic resonance imaging (MRI) is a rapid and non-invasive imaging technique commonly used in hospitals. It investigates the anatomy structure of the body (especially the brain) in both health and disease. The main advantage is that it can provide rich information for either clinical diagnosis or medical research [1]. Soft tissue structures obtained by MRI are more clear and detailed than any other imaging modalities such as CT, Ultrasound, PET, X-ray, etc. [2, 3]. Some researchers are continuously working on MRI in order to improve the quality of magnetic resonance (MR) images, while others are

* Address for correspondence: Yudong Zhang, School of Computer Science and Technology, Nanjing Normal University, Nanjing, Jiangsu 210023, China. Tel.: +86-15905183664; Email: zhangyudong@njnu.edu.cn.
Shuihua Wang, School of Computer Science and Technology, Nanjing Normal University, Nanjing, Jiangsu 210023, China. Tel.: +86-15905183664; Email: wangshuihua@njnu.edu.cn.

to develop novel computer-vision based systems for easy and quick diagnosis [4, 5].

Traditionally, diagnosis results are obtained manually, which were expensive, tiresome, lengthy, and unreliable. The reason may contribute to the too large dataset. This necessitated the requirement to design an automatic and effective computer-aided diagnosis (CAD) tool.

Recently, a mass of methods were proposed for automatic diagnosis. Chaplot, et al. [6] may be the first explorer. They used the approximation coefficients from discrete wavelet transform (DWT) decomposition, and employed both support vector machine (SVM) and self-organizing map (SOM) neural network. However, their research is a bit rough. El-Dahshan, et al. [7] extracted all coefficients from DWT, reduced them by principal component analysis (PCA). Then they used feed-forward back-propagation artificial neural network (FP-ANN) and K-nearest neighbor (KNN) for classification. The FP-ANN and KNN achieved accuracy of 97% and 98%, respectively. However, the classification performance can be improved. Wu and Wang [8] proposed using DWT, PCA, and feed-forward neural network (FNN) trained by scaled chaotic artificial bee colony (SCABC) for feature extraction, for feature reduction, and for classification. Afterwards, Zhang and Wu [9] proposed to use kernel SVM as classification method, and found the GRB kernel achieved the highest accuracy of 99.38%. The prediction time of a 256x256 image was only 0.0448s. Saritha, et al. [10] was the first to employ wavelet-entropy (WE). Besides, they employed spider-web-plot (SWP) to decrease the number of features, and finally employed the probabilistic neural network (PNN). The classification accuracy was found to be 100% on a 75-image dataset with four diseases. The size of dataset was small and the number of categories of diseases is too little. Zhang, et al. [11] suggested that remove spider-web-plot yielded the same classification performance. Das, et al. [12] proposed Ripplet transform (RT) with PCA and with least square SVM (LS-SVM), and their 5x5 CV showed high classification accuracy of 99.39% over a 255-image dataset. Zhang, et al. [13] suggested using particle swarm optimization (PSO) to train the KSVM, and their result on a 90-image database achieved 97.78% accuracy. Kalbkhani, et al. [14] used a Generalized Auto-Regressive Conditional Heteroscedasticity (GARCH) to model the detail coefficients of a 2-level DWT. GARCH's parameters were regarded as the most important feature vector. El-Dahshan, et al. [15] segmented the MR image by the feedback pulse-coupled neural network. Then, they employed the DWT for features extraction, the PCA for reducing the dimensionality of the features, and the FBPNN to classify inputs into pathological or abnormal. The accuracy achieved 99% on a 101-image dataset. Wang and Dong [16] presented a diagnosis method to distinguish Alzheimer's Disease (AD) and mild cognitive impairment (MCI) from normal controls, based on structural MR images by kernel SVM Decision Tree. A 5-fold cross validation showed their method yielded 80% accuracy for these three classes. Zhou, et al. [17] again used wavelet-entropy as the features, and then they employed the Naive Bayes classifier (NBC) for classification. Their results over 64 images showed that the sensitivity reached 94.50%, the specificity 91.70%, the overall accuracy 92.60%. Yang, et al. [18] was the first to use wavelet-energy as the features, and they introduced biogeography-based optimization (BBO) to train the SVM. Their method reached 97.78% accuracy on 90 T2-weighted MR brain images. Wang, et al. [19] used stationary wavelet transform (SWT) as features, and then used FNN as classifiers. However, their computation time is too long. Dong, et al. [20] proposed a novel feature of eigenbrain, and then used machine-learning method to detect AD. Harikumar and Kumar [21] analyzed the performance of ANN, in classification of medical images using wavelets as features. A 96% classification percentage was achieved by the RBF and db4 wavelet. Zhang, et al. [22] proposed a novel classification system that implemented 3D-DWT to extract wavelet coefficients the volumetric image. The triplets (energy, variance, and Shannon entropy) of all subbands coefficients of 3D-DWT were obtained as feature vector. The results showed an overall accuracy of 81.5%.

Although above methods achieved promising results, most of them were vulnerable to following three points: (i) They only considered wavelet coefficients, but did not consider the shape features; and (ii) The classifier did not perform well on new query images. (iii) Their pathological brain detector is not tested on various diseases.

To solve above issues, we suggested two improvements in this paper: (i) We introduced in the wavelet entropy (WE) and Hu moment invariants (HMI), which were good shape features, and (ii) we introduced the generalized eigenvalue proximate SVM (GEPSVM) that was proven of better generalization ability than conventional SVM, and then applied kernel technique to further improve its performance.

2. Wavelet entropy

The famous discrete wavelet transform (DWT) is a powerful signal processing tools that used the dyadic scales and positions for multi-level and multi-resolution analysis [23]. In addition, entropy is a statistical measure of randomness traditionally, which was then redefined as an uncertainty measure for the information content of a system with the definition of $S = -\sum p_j \log_2(p_j)$, where j represents the grey value of reconstructed coefficient, and p_j the corresponding probability.

In this study, we used 2-level haar wavelet, and thus obtained 7 wavelet entropy (WE) features [24] on 7 subband coefficients (LH1, HL1, HH1, LL2, LH2, HL2, and HH2) for each MR brain image.

3. Hu moment invariant

The image shape feature plays a very fundamental role in image classification, so the effective and efficient shape descriptors are the key component of the image representation. We use the image moment as the shape descriptor. For a 2D MR brain image I, the raw moment of order $(m + n)$ is defined as

$$M_{mn} = \sum_x \sum_y x^m y^n I(x, y) \tag{1}$$

where m, $n = 0, 1, 2,\ldots$, and (x, y) the pixel position. The central moments μ are usually used in real applications to replace the raw moment in Eq. (1).

$$\mu_{mn} = \sum_x \sum_y (x - \bar{x})^m (y - \bar{y})^n I(x, y) \tag{2}$$

$$\bar{x} = M_{10}/M_{00}, \bar{y} = M_{01}/M_{00} \tag{3}$$

Note that the central moments are translational-invariant under this definition.

Central moments can be extended to be both translational and scale invariant, by being divided by the scaled (00)-th moment. The results are called normalized central moment.

$$\eta_{mn} = \mu_{mn}/\mu_{00}^{(m+n)/2+1} \tag{4}$$

To enable invariance to rotation, above moments require reformulation. Hu [25] proposed the Hu

moment invariants (HMI). Those expressions were derived from algebraic extensions of the moment-generating function under a pre-set rotation transformation. HMIs consist of a set of nonlinear centralized moment equations, which are also absolutely orthogonal (i.e. rotation) invariant.

4. Classification

In total, 7 wavelet entropy features and 7 Hu moment invariants, i.e., 14 features were submitted to the classification procedure. We established two classifiers: generalized eigenvalue proximal SVM (GEPSVM) and kernel GEPSVM.

Mangasarian and Wild [26] proposed a variant of SVM and termed it as GEPSVM. It avoids the parallelism requirement on the two hyperplanes in conventional SVM, but focuses on forcing minimal the distance from each plane to one of the data sets, and the distance maximal to the other data set. Literatures have shown that GEPSVM excelled standard SVM.

However, traditional GEPSVMs constructed a linear hyperplane to classify data; hence, they failed to solve nonlinear pattern-recognition problem of which a hypersurface is needed; hence, we proposed to apply the kernel strategy [26] to GEPSVM in this study. Radial basis function (RBF) was chosen in this paper because of its extremely good performance reported in various applications.

5. Experiments, results, discussions

In this study, three different ground-truth MR image datasets (Dataset-66, Dataset-160, and Dataset-255) were downloaded from Harvard Medical School for both training and test. The datasets are all T2-weighted MR brain images acquired in axial plane. Their sizes are of 256x256.

The former two datasets were already widely used in research. They consisted of pathological brain images from seven types of diseases together with normal brains. The pathological brain MR images of the former two datasets consisted of following diseases: glioma, meningioma, AD, AD plus visual agnosia, Pick's disease, sarcoma, and Huntington's disease. Recently, Das, et al. [12] proposed a new dataset "Dataset-255", which contains eleven types of diseases. 7 types are also included in the two old datasets, and 4 new diseases (herpes encephalitis, multiple sclerosis, chronic subdural hematoma, and cerebral toxoplasmosis) are added.

Following ease of stratification and common convention, 10x6-fold stratified cross validation (SCV) was used for the first dataset, and 10x5-fold SCV for the rest datasets.

5.1. DWT result

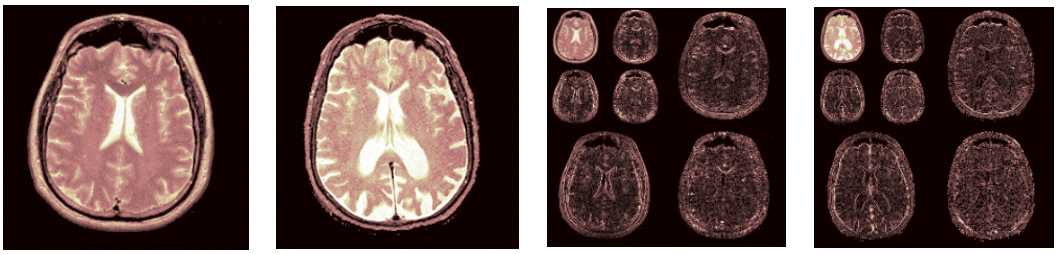

(a) An normal brain (b) An AD brain (c) 2-level DWT of (a) (d) 2-level DWT of (b)

Fig. 1. Wavelet decompositions comparison between normal and pathological brain images.

First, we carried out WE on both a normal and an Alzheimer's disease (AD) MR image, respectively. 2-level Haar wavelet was employed. Fig. 1(a) and 1(b) showed a normal brain MR image and an AD brain MR image. Fig. 1(c) and 1(d) showed the 2-level DWT decomposition results. Pseudocolor of "pink" was rendered for clear view.

5.2. Hu moment invariants

Next, we selected a Pick's brain image, and carried out translation along vertical direction within the range of (-10, 10) with increment of 2, scaling transform with the scaling factor of (0.9, 1.1) with increment of 0.02, and rotation transform with the rotational angle of (-50, 50) with increment of 10. The results were shown in Fig. 2, where the *y*-axis denotes the difference between HMI of transformed image and HMI of original image.

Pictures in Fig. 2 show that the errors are equal to zero at the condition where no transform is performed. The HMIs of transformed image are closely similar to the HMIs of original image; hence, the seven variables of HMI can be regarded as invariant to translation, scaling, and rotation.

5.3. Classification result comparison

We compared the proposed two classification methods (WE + HMI + GEPSVM, and WE + HMI + GEPSVM + RBF), with state-of-the-art methods. The evaluation method was to average the accuracies of *k*-fold SCV. The comparison results are shown in Table 1. The results of existing approaches were extracted from reference [12] with 5 independent runs except that the method "WE + SWP + PNN" was calculated by us with 10 independent runs. All proposed methods ran 10 times to get more robust results.

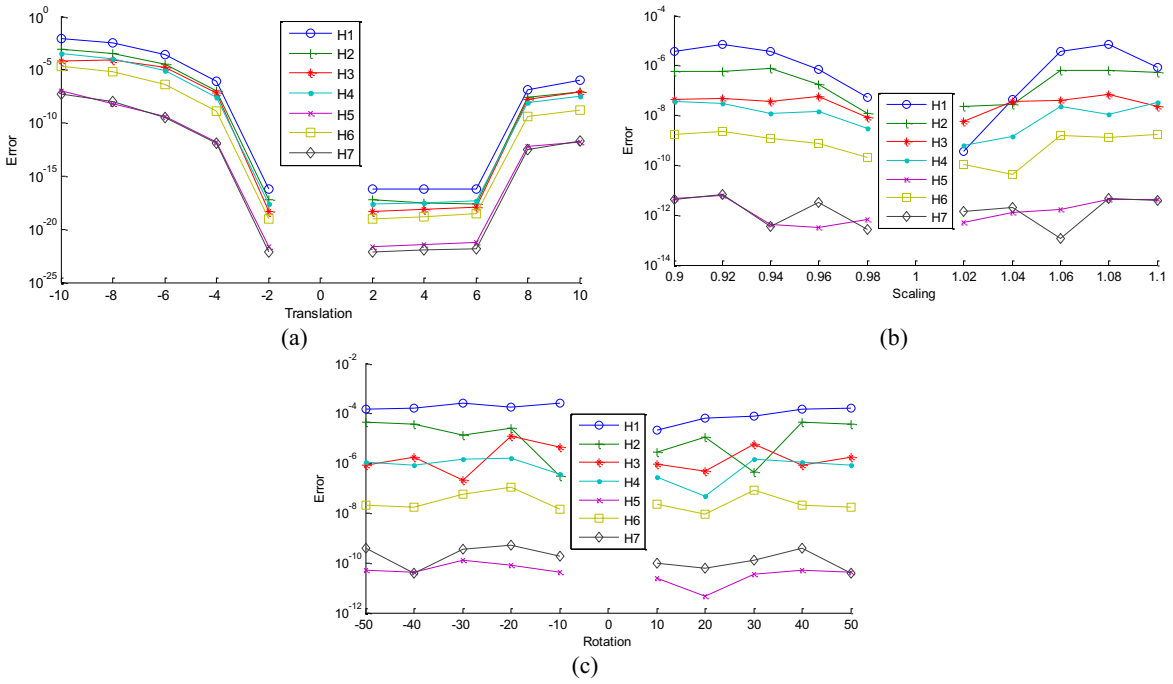

Fig. 2. Validation of invariance of HMI: (a) Translation; (b) Scaling, and (c) Rotation.

Table 1

K-fold classification comparison

Existing Approaches	Dataset-66	Dataset-160	Dataset-255
DWT+SOM [6]	94.00	93.17	91.65
DWT+SVM [6]	96.15	95.38	94.05
DWT + SVM + POLY [6]	98.00	97.15	96.37
DWT + SVM + RBF [6]	98.00	97.33	96.18
DWT + PCA + FP-ANN [7]	97.00	96.98	95.29
DWT + PCA + KNN [7]	98.00	97.54	96.79
DWT + PCA + SVM [9]	96.01	95.00	94.29
DWT + PCA + SVM + HPOL [9]	98.34	96.88	95.61
DWT + PCA + SVM + IPOL [9]	**100.00**	98.12	97.73
DWT + PCA + SVM + GRB [9]	**100.00**	99.38	98.82
WE + SWP + PNN [10]	**100.00**	99.94	98.86
RT + PCA + LS-SVM [12]	**100.00**	**100.00**	99.39
Proposed Approaches	**Dataset-66**	**Dataset-160**	**Dataset-255**
WE + HMI + GEPSVM	**100.00**	99.56	98.63
WE + HMI + GEPSVM + RBF	**100.00**	**100.00**	**99.45**

Table 1 showed the proposed WE + HMI + GEPSVM + RBF obtained classification accuracy of 100.00%, 100.00%, and 99.45% for three datasets, respectively. It outperformed the other proposed diagnosis method (WE + HMI + GEPSVM), which proved the effectiveness of RBF kernel in increasing classification accuracy. Besides, the proposed "WE + HMI + GEPSVM + RBF" excelled existing algorithms. This indicated the accurate prediction of "WE + HMI + GEPSVM + RBF".

The contributions of this paper centered in following aspects. First, we used WE method that offered better information description than conventional DWT method. Second, we applied Hu moment invariants to extract features which were invariant to translation, scaling, and rotation. Third, GEPSVM was employed that had better generalization performance. Fourth, we proved kernel technique was effective in MR brain image classification. Finally, we proved the proposed "WE + HMI + GEPSVM + RBF" method achieved superior accuracy results than other methods.

Indeed, there are two limitations of the proposed method. First, the classifier is built machine-oriented other than human-oriented. The formers yield better classification performance than the latter, however, it is difficult for technicians to understand or interpret what the inner mechanism is. Second, our method does not test brain images generated by different scanners and different protocols. As is known, the intensity distribution of MR images is device- and protocol- dependent.

6. Conclusion

In order to develop an effective and automatic classifier of MR brain images, we proposed using WE to replace conventional discrete wavelet transform method, and introduced 7 HMI features that were invariant to translation, scaling, and rotation. Afterwards, we proposed to use the GEPSVM classifier and suggested to embed RBF kernel. The experiments showed the proposed "WE + HMI + GEPSVM + RBF" method yielded superior performance to existing methods in terms with accuracy over three datasets.

Acknowledgment

This paper was supported by NSFC (610011024, 61273243 and 51407095), Jiangsu Key Laboratory of 3D Printing Equipment and Manufacturing (BM2013006), Program of Natural Science Research of Jiangsu Higher Education Institutions (14KJB520021 and 13KJB460011), Key Supporting Science and Technology Program (Industry) of Jiangsu Province (BE2013012-2, BE2012201 and BE2014009-3), and Nanjing Normal University Research Foundation for Talented Scholars (2014119XGQ0080 and 2013119XGQ0061).

References

[1] S. Goh, et al., Mitochondrial dysfunction as a neurobiological subtype of autism spectrum disorder: Evidence from brain imaging, JAMA Psychiatry **71** (2014), 665-671.
[2] Y. Zhang, et al., Energy preserved sampling for compressed sensing MRI, Computational and Mathematical Methods in Medicine **2014** (2014), 12.
[3] Z. Dong, et al., Improving the spectral resolution and spectral fitting of 1H MRSI data from human calf muscle by the SPREAD technique, NMR in Biomedicine **27** (2014), 1325-1332.
[4] S. Wang, G. Ji and Z. Dong, An improved quality guided phase unwrapping method and its applications to MRI, Progress in Electromagnetics Research **145** (2014), 273-286.
[5] Y. Zhang, et al., Exponential wavelet iterative shrinkage thresholding algorithm with random shift for compressed sensing magnetic resonance imaging, IEEJ Transactions on Electrical and Electronic Engineering **10** (2015), 116-117.
[6] S. Chaplot, L.M. Patnaik and N.R. Jagannathan, Classification of magnetic resonance brain images using wavelets as input to support vector machine and neural network, Biomedical Signal Processing and Control **1** (2006), 86-92.
[7] E.S.A. El-Dahshan, T. Hosny and A.B.M. Salem, Hybrid intelligent techniques for MRI brain images classification, Digital Signal Processing **20** (2010), 433-441.
[8] L. Wu and S. Wang, Magnetic resonance brain image classification by an improved artificial bee colony algorithm, Progress in Electromagnetics Research **116** (2011), 65-79.
[9] Y. Zhang and L. Wu, An MR brain images classifier via principal component analysis and kernel support vector machine, Progress in Electromagnetics Research **130** (2012), 369-388.
[10] M. Saritha, K. Paul Joseph and A.T. Mathew, Classification of MRI brain images using combined wavelet entropy based spider web plots and probabilistic neural network, Pattern Recognition Letters **34** (2013), 2151-2156.
[11] Y. Zhang, et al., Effect of spider-web-plot in MR brain image classification, Pattern Recognition Letters **62** (2015), 14-16.
[12] S. Das, M. Chowdhury and M.K. Kundu, Brain MR image classification using multiscale geometric analysis of ripplet, Progress in Electromagnetics Research-Pier **137** (2013), 1-17.
[13] Y. Zhang, et al., An MR brain images classifier system via particle swarm optimization and kernel support vector machine, The Scientific World Journal **2013** (2013), 9.
[14] H. Kalbkhani, M.G. Shayesteh and B. Zali-Vargahan, Robust algorithm for brain magnetic resonance image (MRI) classification based on GARCH variances series, Biomedical Signal Processing and Control **8** (2013), 909-919.
[15] E.S.A. El-Dahshan, et al., Computer-aided diagnosis of human brain tumor through MRI: A survey and a new algorithm, Expert Systems with Applications **41** (2014), 5526-5545.
[16] S. Wang and Z. Dong, Classification of Alzheimer disease based on structural magnetic resonance imaging by kernel support vector machine decision tree, Progress in Electromagnetics Research **144** (2014), 171-184.
[17] X. Zhou, et al., Detection of pathological brain in MRI scanning based on Wavelet-entropy and naive Bayes classifier, in: Bioinformatics and Biomedical Engineering, F. Ortuño and I. Rojas, eds., Springer International Publishing, Granada, Spain, 2015, pp. 201-209.
[18] G. Yang, et al., Automated classification of brain images using wavelet-energy and biogeography-based optimization, Multimedia Tools and Applications (2015), 1-17.
[19] S. Wang, et al., Feed-forward neural network optimized by hybridization of PSO and ABC for abnormal brain detection, International Journal of Imaging Systems and Technology **25** (2015), 153-164.
[20] Z. Dong, et al., Detection of subjects and brain regions related to Alzheimer's disease using 3D MRI scans based on eigenbrain and machine learning, Frontiers in Computational Neuroscience **66** (2015), 1-15.
[21] R. Harikumar and B.V. Kumar, Performance analysis of neural networks for classification of medical images with wavelets as a feature extractor, International Journal of Imaging Systems and Technology **25** (2015), 33-40.
[22] Y. Zhang, et al., Detection of Alzheimer's disease and mild cognitive impairment based on structural volumetric MR

images using 3D-DWT and WTA-KSVM trained by PSOTVAC, Biomedical Signal Processing and Control **21** (2015), 58-73.
[23] L. Fang, L. Wu and Y. Zhang, A novel demodulation system based on continuous wavelet transform, Mathematical Problems in Engineering **2015** (2015), 9.
[24] Y. Zhang, et al., Preclinical diagnosis of magnetic resonance (MR) brain images via discrete wavelet packet transform with tsallis entropy and generalized eigenvalue proximal support vector machine (GEPSVM), Entropy **17** (2015), 1795-1813.
[25] M.-K. Hu, Visual pattern recognition by moment invariants, IRE Transactions on Information Theory **8** (1962), 179-187.
[26] O.L. Mangasarian and E.W. Wild, Multisurface proximal support vector machine classification via generalized eigenvalues, IEEE Transactions on Pattern Analysis and Machine Intelligence **28** (2006), 69-74.